158P.

Volume 71, number 3,4 OPTICS COMMUNICATIONS 15 May 1989

OPTICAL TRACKING AND MOTION DETECTION USING PHOTOREFRACTIVE $Bi_{12}SiO_{20}$

J.A. KHOURY, G. HUSSAIN [1] and R.W. EASON [1]
Department of Physics, University of Essex, Wivenhoe Park, Colchester, Essex CO4 3SQ, UK

Received 31 October 1988; revised manuscript received 20 February 1989

We demonstrate a technique for the differentiation of time varying optical images that exploits the spatial frequency dependent response time of grating formation in photorefractive BSO. The detection characteristics for such a differential signal can be varied via a tunable response time for each arm of a Michelson interferometer arrangement. Experimental results are presented for various rates of change of the input signal by chopping at different speeds, displacing an input transparency, and directional motion of the object. To illustrate this last operation, results are also presented for the Fourier plane of an output image.

1. Introduction

Robotic vision, security applications and various industrial situations may require the nullification of any static or unchanging portions of an image or scene while highlighting those areas showing motion. This operation has been given the name image differentiation in time [1] and has been achieved to date by the use of computer techniques that subtract a stored image from the current image on a pixel by pixel basis. The current upsurge towards achieving optical analogues of these electronic devices may open up many areas for new optical techniques which could prove more compact, versatile or simple than their conventional counterparts.

An optical tracking novelty filter that performs just such a process of optical image differentiation using an interferometric arrangement involving $BaTiO_3$ has recently been demonstrated [2]. This devices exploits differential optical phase changes and is therefore restricted to highlighting or tracking phase objects only. Other schemes for coherent optical image differentiation based on two beam coupling in $BaTiO_3$ have also been demonstrated [1,3]. These two devices rely on destructive interference between reference and signal beams under static conditions but require high optical quality for the $BaTiO_3$ crystal so that the transmitted images do not suffer from any spatial distortion. In this paper we report a novel arrangement for optical differentiation of images in time that uses an optical processor based on the spatial frequency dependent response time of photorefractive $Bi_{12}SiO_{20}$ in a phase conjugate Michelson interferometric configuration. The device is capable of differentiating both amplitude and phase objects. To our knowledge this is the first time that BSO with its inherent fast response time, some two to three orders of magnitude faster than $BaTiO_3$, has been used for such optical differentiation in time.

2. Theory

Illumination of photorefractive BSO by two or more coherent beams in a spectral region from the uv to near infra-red allows the recording of real time phase volume holograms. The recording mechanism (in diffusion case) is accomplished by the creation of a varying space charge grating which is, in general, out of phase with the illumination grating. This space charge grating is balanced by a corresponding spatially varying electric field in accordance with Poisson's equation. This in turn modulates the refractive index within the crystal volume, through the linear electrooptic effect. Simultaneous multiple gratings can be recorded by the interference of more than one object beam with a common pump beam. A readout

[1] Department of Physics, The University Highfield, Southampton, Hants SO9 5NH, UK.

beam, counter propagating with respect to the pump beam, simultaneously reads out the gratings thereby generating multiple phase conjugate output beams [4]. In photorefractive materials the recording and decay times of a grating depend on several parameters such as grating spacing, total incident light intensity, crystal orientation and any external applied field [5,6]. The erasing time τ_e can be represented through the expression [7],

$$\tau_e = \tau_{di}[1 + f_D(\Lambda) + f_E(\Lambda)E_0^2], \quad (1)$$

where $\tau_{di} = \epsilon\epsilon_0/\sigma$ is the dielectric relaxation time, and σ is the conductivity. E_0 is any externally applied electric field and

$$f_D(\Lambda) = 4\pi\mu\tau_R K_B T/e\Lambda^2,$$

$$f_E(\Lambda) = \frac{4\pi^2 e(\mu\tau_R)^2}{e\Lambda^2 + 4\pi\mu\tau_R K_B T}. \quad (2)$$

Here Λ is the grating fringe spacing, and τ_R is the carrier recombination time. It is clear from the above equations that in the diffusion regime the response time for writing holograms with large fringe spacings is faster than for those with small fringe spacings, while the dielectric relaxation time τ_{di} is inversely proportional to the total incident intensity. By controlling the respective intensity and fringe spacing therefore, the response time of a photorefractive material can be varied. More importantly for several different simultaneous inputs, the response time of each grating can be *independently* tuned for applications such as the differential device described here. The basic requirement for this optical image differentiation in time is the principle of coherent subtraction between two simultaneous phase conjugates under static conditions. For the differential device described here, in practice a suitable combination of angles and relative intensities for the two beams can always be found, thus ensuring complete subtraction.

The technique for subtraction that we use here relies on a phase conjugate Michelson interferometric configuration that has been reported earlier [8,9]. This technique is predicted by the Stoke's relation that holds for a lossless dielectric beam splitter. The intensity at the output port of the dielectric beam splitter can be described by

$$r't^* + r^*t = 0, \quad (3)$$

where r and r' are the amplitude reflection coefficients for the two phase conjugate beams, incident from opposing directions at the beam splitter under conditions of true phase conjugation. Exact image subtraction can be achieved when the intensities of the phase conjugates are equal in both arms of the interferometer. This Stoke's principle has a physical interpretation, which is that under complete time reversal, no input from the image plane to the beamsplitter guarantees no corresponding output. As the input image plane is behind the dielectric beam splitter therefore, any temporal change in the image will be input simultaneously into both arms of the interferometer. Due to the differing response times of each arm however, one phase conjugate output may lag behind the other, and destructive interference will not occur at the beam splitter until a certain time has elapsed. Therefore, in a transient regime the reversibility in time is not valid. During the recording cycle the light amplitude at the output port of the beam splitter BS2 can be written as,

$$A_{out}(x, t) \propto A(x, [t-\tau_1]) - A(x, [t-\tau_2])$$
$$\simeq \partial A(x, t)/\partial t(\tau_{1r} - \tau_{2r}), \quad (4)$$

where τ_{1r} and τ_{2r} are the response times for recording holograms with small and large fringe spacings respectively. Similarly, the output at BS2 during the erasure cycle can be given as

$$A_{out} \approx (\partial A/\partial t)\ (\tau_{1e} - \tau_{2e}), \quad (5)$$

where τ_{1e} and τ_{2e} are the grating decay times for small and large fringe spacings respectively. From equations (4) and (5) above it is evident that the insertion of any time varying signal at the input will result in the output predicted above, corresponding to either the recording cycle or the erasing cycle. Detection of an output signal relies on two factors, the rate of change of the input signal, $\partial A/\partial t$, and the difference in the response time for writing and erasing.

It is not necessary for the interference between the two phase conjugate signals to be destructive, as the amplitudes of the associated space charge fields are (i) not in steady state, (ii) may not have equal magnitude and (iii) the spatial phase shift will not equal $\pi/2$ in a non steady state regime. The temporal development of the output signal is related to the development of amplitudes and phases of the two space

charge fields in time. The difference between the response times of the two gratings may be arbitrarily increased. This can be achieved by either reducing the total intensity of all the interacting beams or the readout beam alone, thereby limiting the differential output to the erasing cycle. Another possibility for increasing the response time difference between the two signals is by using an appropriate wavelength for example orange or red in the case of BSO, since the differentiation will then occur on both writing and erasing cycles.

3. Experimental and results

Fig. 1 shows the experimental arrangement used. A krypton ion laser operating in multilongitudinal mode at 568 nm with a total power I_0 of 14 mW and a single BSO crystal of dimensions 10 mm × 10 mm × 2 mm were used. The beam was spatially filtered, expanded to a diameter of ≈7 mm, and subsequently split by BS1. The transmitted beam was divided by a dielectric beam splitter BS_2 into two input beams I_1 and I_2. A neutral density filter was placed in beam I_1 to reduce the intensity of the conjugate beam to equal that of I_2, and simultaneously to increase the response time of the grating. The measured intensities of the two input beams I_1, I_2 and the pump beam I_3 were 0.8 mW, 1.5 mW and 1.6 mW respectively. The pump beam on passing through the BSO crystal, half wave plate and converging lens L_3 was loosely focussed into the $BaTiO_3$ crystal. The $BaTiO_3$ crystal acts as a self-pumped retroreflector [10], and provides a readout beam that is the exact phase conjugate of I_3. The use of $BaTiO_3$ greatly simplifies the experimental procedure for positioning of counter propagating pumps, and also provides optimum fidelity for the phase conjugate output, as the two pump beams are therefore mutually phase conjugate. Lenses L_1 and L_2 both of 300 mm focal length were used for 1:1 imaging of the input transparency into the crystal and of the phase conjugate to the image plane respectively. Beam I_1 was at an angle of 50° and beam I_2 at an angle of 7° with respect to the pump beam. Under the optimum conditions of overlap, two independent phase conjugates were obtained free of crosstalk. The two phase conjugates were subsequently recombined at BS2 to produce mutual cancellation at the output.

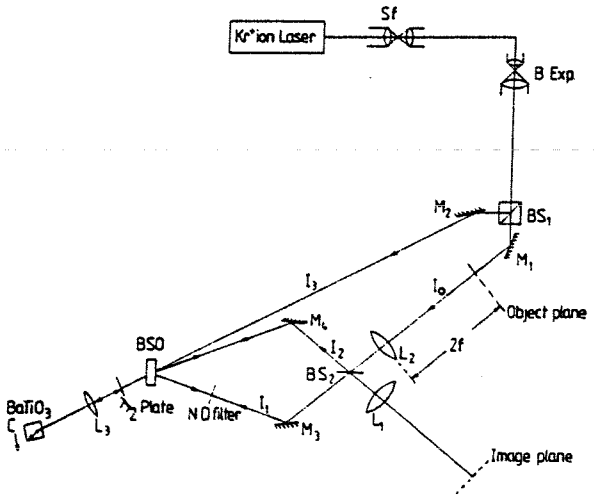

Fig. 1. The experimental arrangement for Optical Motion Detection.

Fig. 2 illustrates a basic operation of the device when the input beam I_0 was subject to chopping at a low frequency (1 Hz). Figs. 2(a) and 2(b) show the phase conjugates of beams I_1 and I_2 respectively when the input was static (unchopped); fig. 2(c)

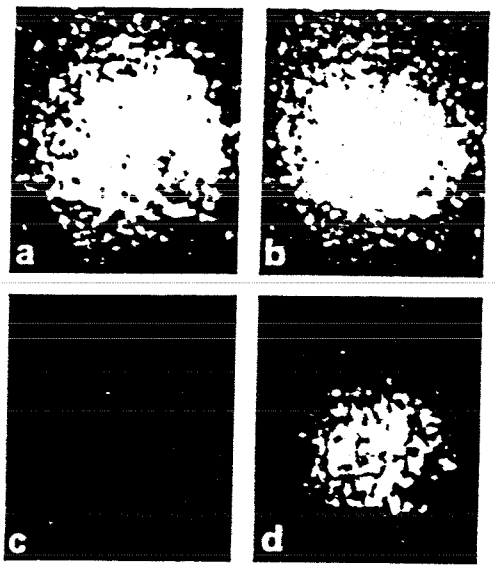

Fig. 2. Basic operation of the device. (A) Phase conjugate of beam I_1. (B) Phase conjugate of beam I_2. (C) Mutual cancellation of both beams under static conditions. (D) Output in the image plane when beam I_0 is chopped at a frequency of 1 Hz.

shows the resultant image subtraction obtained from the output port of BS2 at the image plane, in which almost completely destructive interference has been obtained. When I_0 was chopped however, the variation of response time for beams I_1 and I_2 does yield an output in the image plane, fig. 2(d), as completely destructive interference no longer occurs. It is clear therefore that any temporal change in the object plane may be observed as an output in the image plane.

Using an input wavelength of $\lambda = 568$ nm, and at the low intensities available, the results shown in fig. 2 were obtainable up to a maximum chopping frequency of ≈ 10 Hz. Above this the rise time for grating formation for both beams was sufficiently long that no image was obtained at the image plane. When the $\lambda = 520.8$ nm green line was used however, the maximum chopping rate at which almost complete subtraction occurred extended to ≈ 50 Hz. Between ≈ 70 Hz and ≈ 130 Hz, incomplete destructive interference occurred, and the phase conjugate for one beam only appeared at the image plane.

Fig. 3 shows twelve oscilloscope traces, recorded on a digital storage scope, of the light arriving at a photodiode placed at the image plane, when chopping of beam I_0 occurred at 1, 5 and 10 Hz respectively. In the figure, the first column (A) shows the output from the interferometer arm whose response time was slower, while (B) shows the output from the "faster" arm. In each case these traces were recorded with the other arm blocked. Traces (C) show the results from the output port of BS2 at the image plane when both phase conjugates interfere at BS2, and traces (D) show the residual noise detected by the photodiode when the readout beam was blocked. This represents the amount of scattering, largely from the crystal surface, that was the main problem encountered in trying to achieve complete cancellation at BS2. All the data shown was recorded at $\lambda = 568.2$ nm.

At a 1 Hz chopping rate, which is close to the response time of BSO at this wavelength and input power density, fig. 3(a), for the slower arm, shows that the intensity of the phase conjugate neither saturates nor decays completely during the chopping cycle, whereas in fig. 3(b) the faster response results in a conjugate output that follows the chopping profile much more accurately. Fig. 3(c) is the output at the image plane which results from interference of the two conjugates at BS2. Analysis of this profile is complicated, as we mentioned earlier, for several reasons: the temporal development of both amplitude and phase of the two space charge fields is not independent, and mutual depletion must also occur during this non-steady-state regime. The profile here also has a contribution from the scattering that is seen in fig. 3(d).

At chopping rates of 5 Hz (figs. 3(e)–3(h)) and 10 Hz (figs. 3(i)–3(l)), the results while qualitatively similar, show distinct differences at 5 Hz, the slower arm (3(e)) can clearly no longer follow the rate of chopping. The output is smoothed *or averaged* and the contribution from noise is more apparent than at 1 Hz. The faster arm (3(f)) has an output that appears more saw-toothed than at 1 Hz, again due to the incomplete growth and decay of the conjugate. At 10 Hz, the effect of the increased chopping rate is to reduce the output from the slower arm (3(i)) to effectively a low dc component, and to reduce the output from the faster arm to resemble that in 3(a). Comparing 3(a) with 3(j) therefore we see the ratio of the response times for "fast" and "slow" arms to be roughly 1:10. The corresponding output from BS2 as shown in fig. 3(k) shows very little apart from the scattered noise contribution. When a TV camera is exchanged for the photodiode at this chopping rate, very low output is observed other than noise, a situation which holds for all higher chopping speeds.

The performance of this device was also studied when a resolution test chart was placed in the object plane shown in fig. 1. Fig. 4(A) is the conjugate image from beam 1 of the interferometer (with beam 2 blocked), and 4(B) the result of static cancellation as viewed in the image plane. When the test chart was moved slowly, or temporarily displaced, a bright image transiently appeared fig. 4(C), which disappeared again when static conditions resumed.

Directional motion was also examined, by slowly translating the object in one direction only. Fig. 5(A) and 5(B) show a different part of the test chart under conditions similar to those in fig. 4. When the chart was translated slowly in the x-direction (horizontally), the output mainly consists of those features which are in the y-direction (vertical). Although the quality of these results in poor, it does

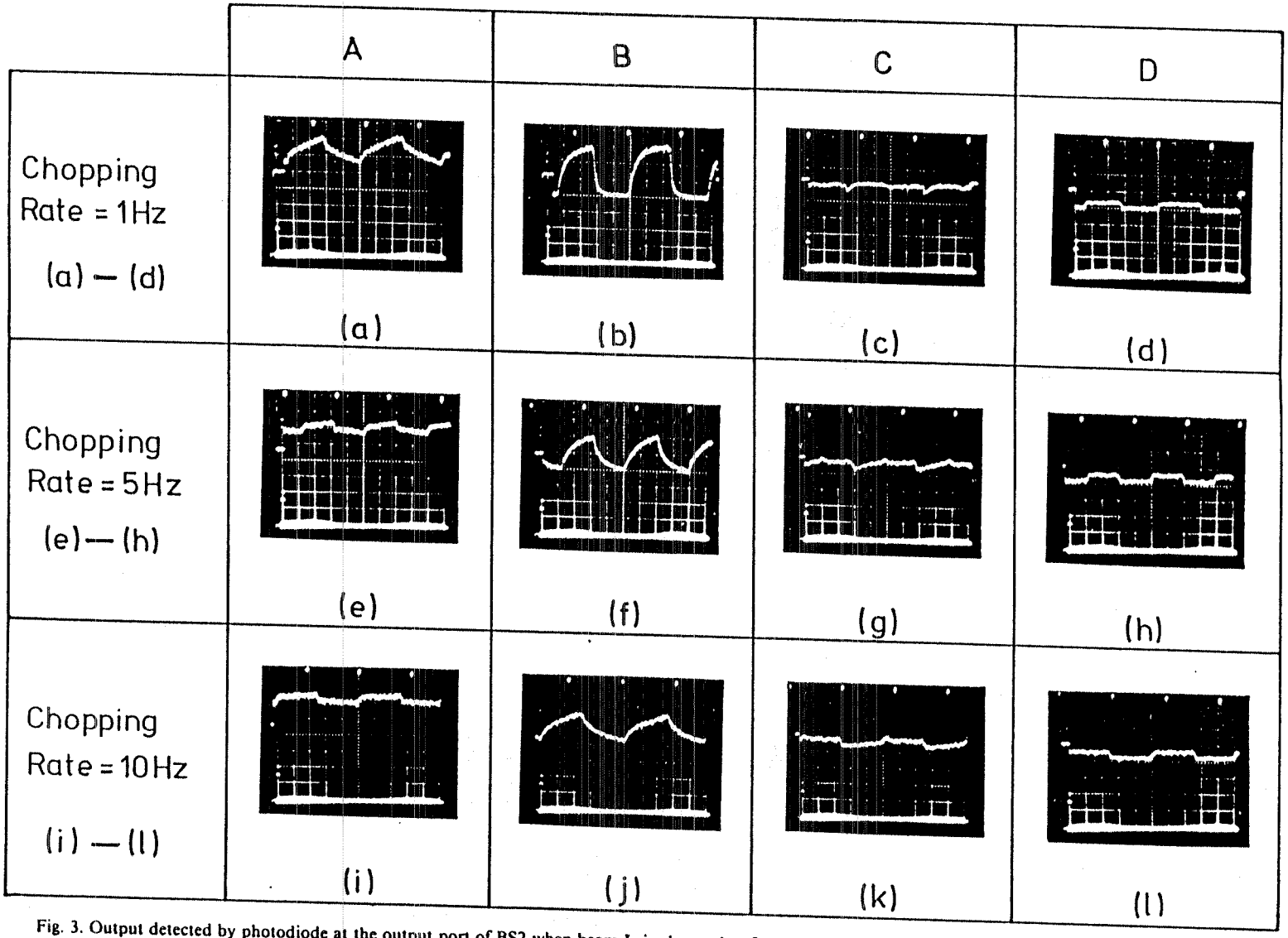

Fig. 3. Output detected by photodiode at the output port of BS2 when beam I_0 is chopped at frequency of 1 Hz, 5 Hz and 10 Hz. (A) and (B) are the phase conjugates of beam I_1 and I_2 respectively. Transient interference between both beams is shown in (C). (D) shows the scattered background light (noise) during the chopping of I_0.

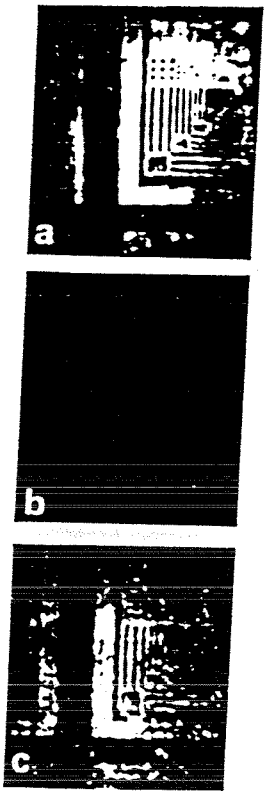

Fig. 4. Photograms showing the response of system to sudden motion in the object plane. (A) Output image of part of test chart from one of the arms of the interferometer. (B) Subtraction of the two images under static conditions. (C) Appearance of the object when displaced slightly from its static position.

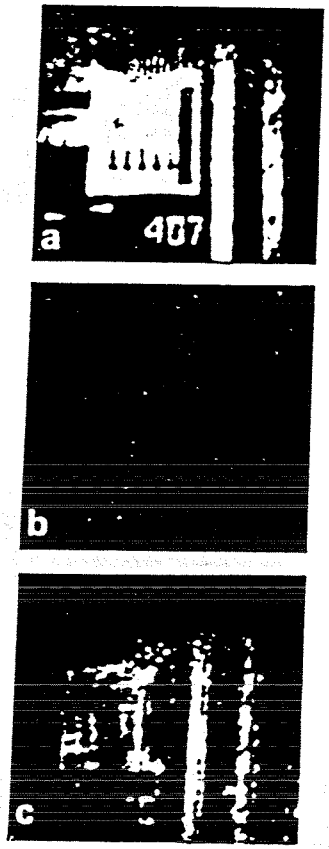

Fig. 5. Results of directional motion of object seen at the image plane. (A) Output from one of the arms. (B) Cancellation of the two images when object is static. (C) Image of the moving object observed at the output port of the BS2.

show the application to spatial differentiation. The difference in response times for each arm results in the appearance of two simultaneous shifted images which are subtracted preferentially in those areas of maximum temporal overlap. The width of the resulting lines, which have a similarity to edge enhanced features, may be used to measure velocity for example. The minimum detectable velocity here would be determined by the minimum between $(\tau_{1e}-\tau_{2e})$ and $(\tau_{1r}-\tau_{2r})$ according to

$$v=\frac{d}{\min[(\tau_{1e}-\tau_{2e}),(\tau_{1r}-\tau_{2r})]},$$

where d is the minimum resolvable feature.

A final technique for observing motion involves examination of the Fourier transform of the information generated via interference at BS2 and output at the image plane. When a second lens is used to generate the transform of the output, a typical spectrum of the input transparency is observed as shown in fig. 6(A) for beam 1 alone. On static cancellation, fig. 6(B) shows near perfect subtraction for all Fourier orders other than the dc, which is present largely due to the unavoidable residual background noise. In principle, this residual noise content can be quantified, and steps taken, such as index-matching, to reduce these deleterious effects to a minimum. Such steps were not taken here, as clearly further refinement is possible at a later stage. As the chart was translated slowly in the x-direction however, only Fourier orders also in the x-direction appeared, corresponding to those features in the image in the orthogonal y-direction, fig. 6(C). An entirely similar

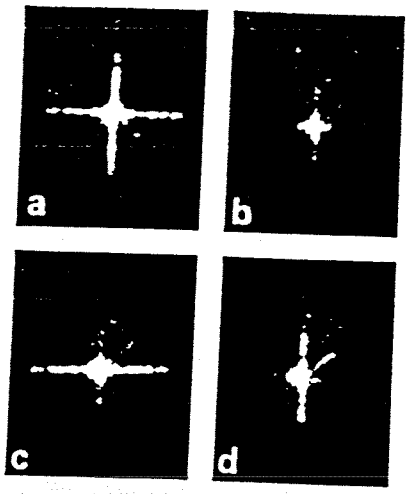

Fig. 6. Fourier transforms of image demonstrating directional filtering. (A) Fourier transform of image from one arm only. (B) Fourier transform of resultant output at image plane under conditions of static cancellation. (C) Output when object undergoes translation in the horizontal direction. Note output is also in horizontal plane. (D) Similar results to (C) above for vertical motion only.

result was obtained for corresponding motion in the y-direction, fig. 6(D).

For fig. 6(C) for example, the number or extent of the Fourier orders that appear is a measure of the speed of translation of the original object. The greater the speed, the less orders appear. This technique has a clear application in directional filtering or velocity selection of moving objects.

4. Conclusion

A technique for optical motion detection and image differentiation in time is described that uses the variable response time of grating formation in two arms of a BSO phase conjugate Michelson interferometer. This allows tunability in the characteristics of the device, for programmable velocity filtering for example. The device is sensitive to temporal changes of amplitude as well as phase for the input image. Future work will concentrate on insertion of real time images via a spatial light modulator.

References

[1] M. Cronin-Golomb, A.M. Biernacki, C. Lin and H. Kong, Optics Lett. 12 (1987) 1029.
[2] D.Z. Anderson, D.M. Liniger and J. Feinberg, Optics Lett. 12 (1987) 128.
[3] R.S. Cudney, R.M. Pierce and J. Feinberg, Nature 332 (1988) 424.
[4] N.A. Vainos and R.W. Eason, Optics Comm. 62 (1987) 131.
[5] G. Valley and M.B. Klein, Opt. Eng. 22 (1983) 704.
[6] P. Gunter, Phys. Rep. 93 (1983) 199.
[7] J. Strait and A.M. Glass, J. Opt. Soc. Am. B 3 (1986) 342.
[8] N.A. Vainos, J.A. Khoury and R.W. Eason, Optics Lett. 13 (1988) 503.
[9] A.E. Chiou and P. Yeh, Optics Lett. 11 (1986) 306.
[10] J. Feinberg, Optics Lett. 7 (1982) 486.